Accepted Manuscript

Effect of applied pressure on microstructure development and homogeneity in an aluminium alloy processed by high-pressure torsion

Piotr Bazarnik, Barbara Romelczyk, Yi Huang, Malgorzata Lewandowska, Terence G. Langdon

PII: S0925-8388(16)32183-1

DOI: 10.1016/j.jallcom.2016.07.149

Reference: JALCOM 38318

To appear in: *Journal of Alloys and Compounds*

Received Date: 4 May 2016

Revised Date: 13 July 2016

Accepted Date: 15 July 2016

Please cite this article as: P. Bazarnik, B. Romelczyk, Y. Huang, M. Lewandowska, T.G. Langdon, Effect of applied pressure on microstructure development and homogeneity in an aluminium alloy processed by high-pressure torsion, *Journal of Alloys and Compounds* (2016), doi: 10.1016/j.jallcom.2016.07.149.

Submitted to Journal of Alloys and Compounds (April 2016): revised July 2016

Effect of applied pressure on microstructure development and homogeneity in an aluminium alloy processed by high-pressure torsion

Piotr Bazarnik[a*], Barbara Romelczyk[a], Yi Huang[b], Malgorzata Lewandowska[a], Terence G. Langdon[b,c]

[a] Warsaw University of Technology, Faculty of Materials Science, Woloska 141, 02-507 Warsaw, Poland

[b] Materials Research Group, Faculty of Engineering and the Environment, University of Southampton, Southampton SO17 1BJ, UK

[c] Departments of Aerospace & Mechanical Engineering and Materials Science, University of Southern California, Los Angeles, CA 90089-1453, USA

Abstract

An investigation was conducted to evaluate the influence of applied pressure on the processing of an aluminium 5483 alloy by high-pressure torsion (HPT). Discs were processed by HPT through 1/4 to 5 revolutions at room temperature using the two different applied pressures of 1.0 and 6.0 GPa. Samples were examined after HPT using microhardness measurements and transmission electron microscopy. Colour-coded maps were constructed to show the hardness distributions and the mechanical properties were evaluated by tensile testing. It is shown that the results are dependent upon the applied pressure such that a higher pressure enhances the accumulation of defects and leads to a more rapid grain refinement. The effect of pressure is especially visible in the early stages after fractional numbers of turns since the microstructure and properties tend to homogenize at high numbers of turns.

Keywords: Al-Mg alloy; Applied pressure; Grain refinement; High-pressure torsion; Microhardness.

[*]Corresponding author: Piotr Bazarnik (p.bazarnik@inmat.pw.edu.pl)

1. Introduction

The processing of bulk metallic samples through severe plastic deformation (SPD) methods provides an opportunity for achieving exceptional grain refinement, even to the nanometer level [1-5], and this produces a very substantial increase in the mechanical strength. Although a number of SPD processing techniques are now available [6-9], most attention has centred on the use of either equal-channel angular pressing (ECAP) where a rod or bar is pressed through a special die [10] or high-pressure torsion (HPT) where a disk is subjected to a high applied pressure and concurrent torsional straining [11]. In practice, experiments show that HPT is the optimum processing procedure because, by comparison with ECAP, it leads both to smaller grains [12,13] and to a larger fraction of grain boundaries having high angles of misorientation [14]. For example, experiments on an Al-5% Mg alloy gave a grain size of ~70 nm when processing by HPT at room temperature [5].

In HPT processing, the applied strain is a major parameter influencing the process of grain refinement and the final microstructure. However, the equivalent von Mises strain, ε_{eq}, imposed during torsional straining is given by a relationship of the form [15]:

$$\varepsilon_{eq} = \frac{2\pi N r}{h\sqrt{3}} \tag{1}$$

where N is the number of revolutions and r and h are the radius and height (or thickness) of the disc, respectively. It is readily apparent from Eq. (1) that there is zero strain at the centre of the disc and then a linear increase so that the strain is a maximum at the edge of the disc. It is reasonable to anticipate from Eq. (1) that the microhardness and the microstructure will be strongly inhomogeneous in HPT samples and specifically they will depend upon the precise location within the disc. In practice, however, this is true only in the initial stages of processing and after a sufficiently high number of HPT revolutions both the hardness and the microstructure generally become reasonably homogeneous both across the disc surfaces [16,17] and through the vertical cross-sections of the HPT discs [18]. This evolution is

consistent with the predictions of the HPT processing from strain gradient modelling [19]. Generally, and with only a small number of exceptions, the microstructure ultimately attains a steady-state condition and this is consistent with a saturation in the microhardness which becomes apparent when the individual microhardness datum points are plotted as a function of the equivalent strain [20-23].

It is also anticipated that the applied pressure may have an effect on the microstructural development since the imposition of pressure in HPT prevents crack formation and segmentation in the processing of hard-to-deform materials [24]. This high pressure is also crucial for generating frictional forces that are sufficiently high to firmly hold the samples and allow torsion straining without the occurrence of any slippage [25]. There are reports documenting the development of convex curvatures on the surfaces of discs after HTP processing [26,27] and recently it was shown through finite element modelling that this is a consequence of the elastic deformation of the anvils during the processing operation [28]. It was noted also that the thickness variations in the HPT samples depend upon the maximum applied pressure during processing. This shape change takes place during the initial compression stage in HPT because material is forced outwards between the anvils around the periphery of the disc and the amount of this extrusion increases with increasing imposed pressure. This phenomenon is well known and has been adequately described using finite element analysis [29]. More important in the context of the present investigation are the stress-strain distributions within the sample. Specifically, the model shows that the effective stress and strain in the central regions of the compressed discs increase with pressure as a consequence of the frictional forces acting on the disc surface which influence the plastic deformation and hardening behaviour of the material.

The general conclusion from these earlier analyses is that the magnitude of the applied pressure will influence the macroscopic behaviour of samples during HPT processing and it

will also affect the generation of defects and the overall microstructural evolution. For example, the generation of point defects is associated with an increase in volume of the material and the presence of a compressive stress will hinder this process by reducing their formation and mobility rates and hence decreasing the rate of dynamic recovery [29,30]. Also, the energy of dislocation formation will be increased due to changes in the shear modulus G, Poisson ratio ν and the magnitude of the Burgers vector **b**. Earlier reports demonstrated that the applied pressure facilitates the homogenization of the microstructure and the microstructural properties such that a higher pressure leads to less inhomogeneity across the disc radius and thereby facilitates the development of a reasonable level of homogeneity after lower numbers of turns [13,31]. Nevertheless, detailed experiments with an Al-6061 alloy using applied pressures of either 1.25 or 4.0 GPa showed the high hardness values recorded at the outer edges of the discs were reasonably independent of the applied pressure but the extent of this region of high hardness was dependent upon both the applied pressure and the number of torsional revolutions [32].

These earlier results on the Al-6061 alloy were limited exclusively to measurements of the microhardness on the upper surfaces of the discs. Accordingly, the present investigation was initiated to provide a more comprehensive evaluation of the effect of the applied pressure in HPT processing by examining the hardness values on both horizontal and vertical sections within the HPT discs, by conducting detailed microstructural observations and by examining the mechanical properties through tensile testing at room temperature using miniature samples cut from discs after HPT processing.

2. Experimental material and procedures

The experiments were conducted using an aluminium Al-5483 alloy containing 5 wt% of magnesium where the material was received in the form of hot-extruded 50 mm diameter bars. This type of alloy has a high ability to accumulate plastic deformation and produce very

fine grain size structures. The alloy does not exhibit age hardening behaviour which implies that the grain size will be the major strengthening mechanism. For HPT processing, a wire electric discharge machine (EDM) was used to cut discs with diameters of 10 mm and thicknesses of ~0.8 mm.

The HPT processing was conducted at room temperature under quasi-constrained conditions where there is a small outflow of material around the periphery of the disc during the processing operation [26,27,33]. Discs were torsionally strained by rotating the lower anvil at 1 rpm through 1/4, 1/2, 1, 3 and 5 revolutions. In order to determine the influence of pressure on the microstructure and mechanical properties, the HPT processing was conducted under separate applied pressures of either 1.0 or 6.0 GPa.

After HPT processing, hardness tests were conducted on the polished surfaces of discs using an FM-300 microhardness tester equipped with a Vickers indenter. Measurements were taken under a load of 100 g and a dwell time of 10 s along diameters randomly selected across each disc with a spacing of 0.3 mm between the measuring points. In order to provide a comprehensive overview of the influence of the HPT processing parameters on the homogeneity of the structure, detailed microhardness measurements were also taken over the total surfaces of the polished middle sections of selected discs by following a rectilinear grid pattern and recording the hardness values with separations of 0.3 mm between each measuring point. Finally, discs were sectioned vertically and hardness measurements were recorded after polishing on one-half of each cross-sectional plane following a rectilinear grid pattern with a spacing of 0.1 mm between measuring points. The results recorded on the central planes and the one-half cross-sectional planes were then plotted in the form of colour-coded displays of the hardness variations following the procedures introduced earlier for achieving simple visual displays of the hardness variations in ECAP [34] and HPT [16,17].

The mechanical properties were investigated after HPT processing by conducting tensile tests at room temperature. Using EDM, two miniature tensile samples with gauge lengths of 1.0 mm were cut from each disc from off-centre positions located 2.5 mm from the central points as shown in Fig. 1, where the centre of each disc was not included in order to avoid any inhomogeneities that may exist in the vicinity of this central region [36]. Tensile tests were conducted using a Zwick/Roell 005 testing machine at an initial strain rate of 1.0×10^{-3} s^{-1}. The engineering strain was continuously tracked using optical non-contact displacement measurements and Digital Image Correlation (DIC) [37].

The internal structures of each disc were examined using a scanning transmission electron microscope (STEM) Hitachi 5500 operating at 30 kV and a transmission electron microscope (TEM) JEOL 1200 EX operating at 120 kV. Microstructures were examined in the central region of each disc and at points about 3.5 mm from the disc centres to represent the edge regions. The TEM samples were prepared using twin-jet electro-polishing at 5°C. with an electrolytic solution of 30% of HNO_3 and 70% of CH_3OH. Selected-area electron diffraction (SAED) patterns were recorded from regions having diameters of 5 µm.

3. Experimental results

3.1 Variations of microhardness across surface disc diameters

The values of the Vickers microhardness recorded across the surface disc diameters are shown in Fig. 2 where the lower dashed line denotes the initial hardness prior to HPT processing. For simplicity in presentation, data are shown only for samples processed by HPT through 1/4 and 5 revolutions under imposed pressures of 1.0 and 6.0 GPa. These samples show typical increases in hardness relative to the initial condition but the hardness values depend critically on the numbers of HPT revolutions. Furthermore, these measured values tend to be highly non-uniform across the diameters of the samples for low numbers of turns

but there is a transition to a reasonable degree of homogenization after higher numbers of turns with a hardness plateau at Hv ≈ 215.

Close inspection shows that the microhardness values at any selected condition depend only slightly on the applied pressure. Thus, an increase in applied pressure from 1.0 to 6.0 GPa produces a small but measurable increase in the Hv values after 1/4 turn but at 5 turns both pressures give essentially the same values for Hv and the two sets of hardness data are almost coincident. After 5 turns, the results from both pressures show that lower hardness values are recorded in the central region over a diameter of ~2 mm and this is identical for both 1.0 and 6.0 GPa.

3.2 Variation of microhardness values across horizontal and vertical sections

Fig. 3 and 4 show the influence of applied pressure on the microhardness distributions for discs subjected to 1/2, 1 and 3 revolutions under pressures of 1.0 and 6.0 GPa in the disc central plane and in vertical cross-sectional planes, respectively. All of these microhardness values are plotted as colour-coded contour maps where the linear coordinates *X* and *Y* denote two arbitrary axes selected as the orthogonal coordinate system and the hardness values are indicated by the scales on the right. These displays provide direct evidence that the applied pressure affects the local values of the microhardness. Thus, it is evident in Fig. 3 that the discs processed with the smallest numbers of turns of 1/2 and 1 show central regions of lower hardness that extend over wider diameters than in the discs processed with a pressure of 1.0 GPa. In addition, there are local inhomogeneities which are uniformly distributed across the disc surfaces up to 3 turns for both applied pressures although these local inhomogeneities are greater in the disc processed to 1 turn under a pressure of 1.0 GPa.

In Fig. 4 there are differences between the tendencies towards higher hardness values and these differences depend upon the applied pressure. In general, the results confirm that the local hardness values recorded on the vertical cross-sections are generally comparable

with those on the horizontal surfaces but again the distributions of hardness values across the cross-sections depend on the applied pressure. Thus, processing under an upper pressure of 6.0 GPa leads to significant hardening throughout the discs with lower hardness values in the centres and a gradual increase of hardness towards the edges. In practice, it is apparent that the hardness values are fairly uniform across the disc thicknesses. A hardening behaviour is also observed when processing under a pressure of 1.0 GPa but the evolution through the disc thickness tends to be more inhomogeneous. This trend is especially visible after 1 and 3 revolutions where there is a significant variation between the central and upper/lower surfaces of the discs. In general, the highest values of hardness are observed in the central portion of the sample.

3.3 Microstructural observations after HPT

The microhardness measurements were supplemented by examining the microstructures by TEM in the central and outer parts of each disc. Representative examples are shown in Fig. 5 where the applied pressures are 1.0 GPa in the left column and 6.0 GPa in the right column, the two upper rows are for the centre after 1/2 and 5 turns and the two lower rows are for the edge after 1/2 and 5 turns. The results also include the SAED patterns for each processing condition. Quantitative measurements of the grain sizes are summarized in Table 1 for all processing conditions.

Up to 1 revolution there was no significant grain refinement in the central regions at either applied pressure and the mean grain size appeared reasonably consistent with the grain size of ~25 μm in the as-received sample. Nevertheless, the density of dislocations increased when compared with the as-received material and these dislocations were essentially uniformly distributed within the grains. It is important to note the differences between samples processed under these two applied pressures. As the number of revolutions increases, the structure in the central region starts to evolve and after one revolution under a pressure of

6.0 GPa there were some regions of grain refinement showing ultra-fine grains. By contrast, under a pressure of 1.0 GPa there was only a high fraction of dislocations and slip bands after 1 turn. These differences are readily apparent in Fig. 6(a) for 1.0 GPa and Fig. 6(b) for 6.0 GPa.

At the edges of the discs, the structures were highly deformed and significant grain refinement occurred in these regions at both pressures even after only 1/2 turn as shown in Fig. 5. Thus, the average grain sizes were reduced to ~170 and ~155 nm for pressures of 1.0 and 6.0 GPa, respectively. These ultrafine grains were reasonably equiaxed and the azimuthal spreading of spots in the SAED patterns indicated the presence of high internal stress in these regions. This suggests that a major proportion of the grain boundaries have low angles of misorientation. A detailed analysis of the grain sizes showed a visible difference in the samples processed through a fractional number of revolutions. Thus, grain size measurements near the edge in the samples processed by 1/4 turn gave mean grain sizes of ~200 and 170 nm after processing under pressures of 1.0 and 6.0 GPa, respectively. All of these early measurements show a potential for achieving greater grain refinement at higher applied pressures in the very early stages of HPT processing whereas after 5 turns the measured average grain sizes were similar at ~110 and ~120 nm after processing at 1.0 and 6.0 GPa, respectively.

It is readily evident from Fig. 5 that processing through 5 revolutions was sufficient to form a homogeneous structure throughout the samples. However, for both applied pressures there was a small but significant difference in the average grain sizes measured in the central and edge regions as shown in Table 1 where the grain sizes in the central region after 5 turns were ~250 and ~235 nm at 1.0 and 6.0 GPa, respectively. It is also apparent from Table 1 that this difference in grain size tends to decrease with increasing numbers of turns and after 3 turns the microstructures were similar but there was a small difference in grain size. Also, a

detailed analysis of the SAED patterns showed that the diffraction spots are more spread towards rings in the samples processed under the higher pressure and this suggests that higher pressures produce arrays of ultrafine grain having larger differences in the orientations so that high pressures are more effective in producing grain boundaries having higher misorientation angles.

3.4 Tensile properties after HPT processing

To investigate the effects of the different initial microstructures on subsequent tensile testing, tensile tests were conducted only for samples processed up to 3 revolutions. The results are shown in Fig. 7 for pressures of (a) 1.0 and (b) 6.0 GPa and the properties are recorded in Table 2 for the ultimate tensile strength (UTS) and the yield strength (YS). For the as-received material, there was an initial YS of ~145 MPa and a UTS of ~285 MPa. Thus, the grain refinement achieved in HPT processing led to significant increases in the YS and UTS after both low and high numbers of revolutions for both applied pressures.

Inspection of the stress-strain curves in Fig. 7 show that the tensile characteristics are different when considering the effect of pressure. After 1/4 revolution both samples have similar UTS at a level of ~500 MPa but with increasing numbers of turns the mechanical properties of samples processed at 1.0 GPa increase only slightly whereas there is a larger increase in the samples processed at 6.0 GPa. This difference is especially evident after 1 turn where the sample processed at 6.0 GPa has a UTS which is ~180 MPa higher than after processing at 1.0 GPa. This difference in the mechanical properties decreases with increasing numbers of turns and after 3 revolutions both samples exhibit similar tensile characteristics and show very high strengths exceeding 800 MPa but with little or no ductility.

4. Discussion

4.1 The Al-Mg alloy after SPD processing

The results from this study show that HPT processing leads to a significant strain hardening in the aluminium 5483 alloy even processing through only 1/4 turn. The hardening behaviour observed in this alloy, as depicted in Fig. 3, fits into the hardening model without recovery as described in a comprehensive review of the different models of hardening evolution in ultrafine-grained (UFG) metals processed by HPT [38]. This type of hardening differs from pure aluminium [16] where the initial hardening is followed by softening prior to stabilising at a saturation condition. This softening is due to the high stacking fault energy (SFE) in pure aluminium and therefore the relative ease of recovery through cross-slip of the screw dislocations. The lack of any softening in the Al-5483 alloy, and in other similar aluminium alloys where there is an Mg addition, is due to the lower SFE [39,40] and the consequent hindering of the recovery process. This lack of significant recovery means that more dislocations are stored in the material leading to a smaller grain size. The trend for a decrease in grain size with increasing additions of Mg in aluminium was recognized in very early experiments on the processing of Al-Mg alloys by ECAP where the grain sizes were reduced from ~1.3 μm in pure Al to ~450 and ~270 nm in Al-1% Mg and Al-3% Mg, respectively [41]. This reduction in grain size is consistent also with the higher strength recorded after HPT processing in Fig. 7.

Although it is consistently reported that the strengthening of metallic samples is a direct consequence of the SPD processing [1], the mechanical properties of the present Al-5Mg alloy significantly exceeds the properties reported in less dilute Al-xMg (0.5-4%) alloys processed by various SPD methods [41-48] and it may be compared even with the results obtained from samples containing higher amount of magnesium processed by ECAP [49] or HPT [50]. To place these results in perspective, Table 3 summarizes the mechanical properties of Al-Mg alloys processed by a number of different SPD methods [3,41-56]. A careful review of these data provides clear confirmation that the processing of an Al-5Mg

alloy by HPT produces higher strength and hardness than processing by other SPD techniques such as accumulative roll bonding (ARB) [55], Hydrostatic Extrusion (HE) [3,54] or ECAP [54].

In an attempt to explain the high mechanical properties of the HPT-processed 5483 alloy, the data from Table 3 were plotted in the Hall-Petch coordinates as illustrated in Fig. 8 and, where appropriate, the YS data were estimated using the relationship [57]

$$\sigma_y = Hv/3 \quad (2)$$

In general, it is noted that the data follow a linear dependence between YS and the inverse square root of the grain size but there is significant scattering around the straight line. Nevertheless, the data obtained in the present study lie within the reported data and this confirms that the high mechanical properties of the HPT-processed 5483 alloy is due primarily to the grain refinement.

It is important to note also that the grain size of ~130 nm obtained in this study is one of the smallest grain sizes reported for the 5XXX-series aluminium alloys. Nevertheless, the large scattering in the data suggests that there are secondary factors which may also affect the mechanical properties after SPD processing. It was suggested earlier that the character of the grain boundaries may be important [5]. For example, if there is a high fraction of low-angle grain boundaries (LAGBs), the YS may be reduced by comparison with an alloy having the same grain size but high-angle grain boundaries (HAGBs) because the LAGBs are weaker obstacles for moving dislocation and therefore they are less effective in promoting grain boundary strengthening. This trend is confirmed in the present work because the datum points corresponding to small numbers of turns tend to lie below the trend line in Fig. 8 and these samples will have a higher fraction of LAGBs. Thus, these data demonstrate the potential for achieving different mechanical properties in the aluminium 5XXX-series alloys through combinations of different SPD methods.

4.2 The effect of hydrostatic pressure on the evolution of structure and mechanical properties

The results from this research suggest a small but significant dependence of structural evolution on the imposed pressure. Thus, it is readily apparent that homogeneity is achieved more rapidly when processing with larger applied pressures. In the disc planes as in Fig. 3, the surface area of the central region of lower hardness is visibly smaller when processing at the higher pressure. On cross-sectional hardness maps as in Fig. 4, there is a clear localization of plastic deformation in the central regions of the HPT discs of the 1.0 GPa samples whereas in the 6.0 GPa samples the hardness distributions are more uniform across the discs.

In general, the applied pressure plays a dual role in HPT processing. First, it serves to prevent or minimize the effect of slippage between the discs and anvils [25]. Second, it enhances grain refinement by influencing the generation and accumulation of defects [15]. The plastic deformation is related to the friction coefficient [18,25,58] which depends upon the anvil roughness [59] and the applied pressure. Thus, a low hydrostatic pressure during HPT processing may promote slipping especially during the first revolution when the sample is usually matching to the anvil. Studies on copper processed by HPT under pressures of 2.0 and 6.0 GPa showed a high fraction of slippage (~15%) in the sample processed under 2.0 GPa and a reduction in slippage with increasing applied pressure [57]. In addition, the concentration of plastic flow depends on the degree of friction with the walls of the anvils. For low frictional forces, the plastic flow may concentrate near the mid-plane which will lead to the formation of areas of low deformation near the upper and lower surfaces of the sample. This trend is evident in Fig. 4 for the discs processed at 1.0 GPa where there are regions of local microhardness inhomogeneity on the cross-sectional maps. By contrast, a high imposed pressure leads to a larger frictional force between the anvils and the disc and this reduces the extent of slippage [25].

It should be noted that the imposition of a high pressure may significantly affect the generation of defects and thereby influence the microstructural evolution during HPT processing. Thus, a high pressure will reduce the rate of dynamic recovery by diffusion-controlled mechanisms and this will increase the accumulation of dislocations and enhance the efficiency of grain refinement [15,60]. Under higher applied pressures, the generation of point defects will be suppressed since it is associated with an increase in volume of the material [61]. Also, the energy of forming dislocations increases where this is due to the changes in the shear modulus G, the Poisson's ratio ν and the Burgers vector, **b**. From work hardening theory, the energy of dislocations is associated with their mobility which also determines the plastic deformation process in the material. The mobility of dislocations depends upon the lattice frictional or Peierls-Nabarro forces according to a simple equation of the form [62]:

$$\sigma_{\text{l.frict.}} = \frac{2G}{K}\exp\left(-\frac{2d'}{Kb}\right) \tag{3}$$

where K is a constant equal to 1 for edge dislocation and $(1 - \nu)$ for screw dislocations and d' is the distance between the slip planes. The Peierls-Nabarro forces are strongly dependent upon the shear modulus which increases with increasing compressive pressure. As a result, an increase in pressure should contribute to the accumulations of dislocations and thereby to the grain refinement [15,16,63].

For this reason, the process of grain refinement is more advanced in samples processed under higher pressures as shown by the results from this investigation. The effect of pressure is especially visible after fractional or very small numbers of turns so that, as shown in Fig. 2 for discs processed through 1/4 revolution, the values of the microhardness in the peripheral regions are higher when processing with a pressure of 6.0 GPa than at 1.0 GPa. In the central parts of the discs, refined grains are formed after 1 turn for the disc processed at 6.0 GPa

whereas when processing through 1 turn at 1.0 GPa the central region contains a high dislocation density and slip bands.

5. Summary and conclusions

1. A commercial 5483 Al-5Mg alloy was processed by high-pressure torsion for up to 5 revolutions under two different applied pressures of 1.0 and 6.0 GPa. The results show that the microstructure and microhardness evolves with torsional straining but the hardness values tend to be higher around the edges of the disks and lower in the central region. In addition, the inhomogeneity in the central regions decreases with increasing numbers of revolutions.
2. The results show that the microstructure and microhardness evolution is influenced by the applied pressure to a minor extent. A higher imposed pressure enhances the accumulation of defects and thereby facilitates grain refinement.
3. The effect of pressure is especially visible after fractional numbers of turns. At higher numbers of turns, the microstructure and properties tend to homogenize both across the disc plane and through the disc thickness. The results show disc homogeneity is achieved more rapidly when processing at a higher pressure.

Acknowledgements

This research was financed by the National Science Centre, Poland, within the project PRELUDIUM 7 “Microstructure influence on properties in ultra-fine grained aluminium alloy 5483” under Grant Agreement No. 2014/13/N/ST8/01661 and by the European Research Council under ERC Grant Agreement No. 267464-SPDMETALS. This results are also a part of main authors doctoral dissertation, financed by the National Science Centre, Poland, in the form of doctoral scholarship, Agreement No. UMO-2015/16/T/ST8/00160

References

[1] R.Z. Valiev, R.K. Islamgaliev, I.V. Alexandrov, Bulk nanostructured materials from severe plastic deformation, Prog. Mater. Sci. 45 (2000) 103-189.

[2] A. Loucif, R.B. Figueiredo, T. Baudin, F. Brisset, R. Chemam, T.G. Langdon, Ultrafine grains and the Hall–Petch relationship in an Al–Mg–Si alloy processed by high-pressure torsion, Mater. Sci. Eng. A 532 (2012) 139-145.

[3] P. Bazarnik, B. Romelczyk, M. Kulczyk, M. Lewandowska, The strength and ductility of 5483 aluminium alloy processed by various SPD methods, Mater. Sci. Forum 765 (2013) 423-428.

[4] T.G. Langdon, Twenty-five years of ultrafine-grained materials: Achieving exceptional properties through grain refinement, Acta Mater. 61 (2013) 7035-7059.

[5] P. Bazarnik. Y. Huang, M. Lewandowska, T.G. Langdon, Structural impact on the Hall–Petch relationship in an Al–5Mg alloy processed by high-pressure torsion, Mater. Sci. Eng. A 626 (2015) 9-15.

[6] R.Z. Valiev, Y. Estrin, Z. Horita, T.G. Langdon, M.J. Zehetbauer, Y.T. Zhu, Producing bulk ultrafine-grained materials by severe plastic deformation, JOM 58(4) (2006) 33-39.

[7] A. Azushima, R. Kopp, A. Korhonen, D.Y. Yang, F. Micari, G.D. Lahoti, P. Groche, J. Yanagimoto, N. Tsuji, A. Rosochowski, A. Yanagida, Severe plastic deformation (SPD) processes for metals, Manuf. Tech. 57 (2008) 716-735.

[8] I. Sabirov, M.Y. Murashkin, R.Z. Valiev, Nanostructured aluminium alloys produced by severe plastic deformation: New horizon in development, Mater. Sci. Eng. A 560 (2013) 1-24.

[9] R.Z. Valiev, Y. Estrin, Z. Horita, T.G. Langdon, M.J. Zehetbauer, Y.T. Zhu, Producing bulk ultrafine-grained materials by severe plastic deformation: Ten years later, JOM 68 (2016) 1216-1226.

[10] R.Z. Valiev, T.G. Langdon, Principles of equal-channel angular pressing as a processing tool for grain refinement, Prog. Mater. Sci. 51 (2006) 881-981.

[11] A.P. Zhilyaev, T.G. Langdon, Using high-pressure torsion for metal processing: Fundamental and applications, Prog. Mater. Sci. 53 (2008) 893-979.

[12] A.P. Zhilyaev, B.K. Kim, G.V. Nurislamova, M.D. Baró, J.A. Szpunar, T.G. Langdon, Orientation imaging microscopy of ultrafine-grained nickel, Scr. Mater. 46 (2002) 575–580.

[13] A.P. Zhilyaev, G.V. Nurislamova, B.K. Kim, M.D. Baró, J.A. Szpunar, T.G. Langdon, Experimental parameters influencing grain refinement and microstructural evolution during high-pressure torsion, Acta Mater. 51 (2003) 753–765.

[14] J. Wongsa-Ngam, M. Kawasaki, T.G. Langdon, A comparison of microstructures and mechanical properties in a Cu-Zr alloy processed using different SPD techniques, J. Mater. Sci. 48 (2013) 4653–4660.

[15] R.Z. Valiev, Yu.V. Ivanisenko, E.F. Rauch, B. Baudelet, Structure and deformation behaviour of Armco iron subjected to severe plastic deformation, Acta Mater. 44 (1996) 4705-4712.

[16] C. Xu, Z. Horita, T.G. Langdon, The evolution of homogeneity in processing by high-pressure torsion, Acta Mater. 55 (2007) 203-212.

[17] M. Kawasaki, S.N. Alhajeri, C. Xu, T.G. Langdon, The development of hardness homogeneity in pure aluminum and aluminum alloy disks processed by high-pressure torsion, Mater. Sci. Eng. A 529 (2011) 345-351.

[18] M. Kawasaki, R.B. Figueiredo, T.G. Langdon, An investigation of hardness homogeneity throughout disks processed by high-pressure torsion, Acta Mater. 59 (2011) 308-316.

[19] Y. Estrin, A. Molotnikov, C.H.J. Davies, R. Lapovok, Strain gradient modeling of high-pressure torsion, J. Mech. Phys. Solids 56 (2008) 1186-1202.

[20] S. Sabbaghianrad, T.G. Langdon, A critical evaluation of the processing of an aluminum 7075 alloy using a combination of ECAP and HPT, Mater. Sci. Eng. A 596 (2014) 52-58.

[21] O. Andreau, J. Gubicza, N.X. Zhang, Y. Huang , P. Jenei, T. G. Langdon, Effect of short-term annealing on the microstructures and flow properties of an Al–1% Mg alloy processed by high-pressure torsion, Mater. Sci. Eng. A 615 (2014) 231-239.

[22] M. Kawasaki, Different models of hardness evolution in ultrafine-grained materials processed by high-pressure torsion, J. Mater. Sci. 49 (2014) 18-34.

[23] S. Sabbaghianrad, T.G. Langdon, An evaluation of the saturation hardness in an aluminum 7075 alloy processed using different techniques, J. Mater. Sci. 50 (2015) 4357-4365.

[24] Y. Huang, R.B. Figueiredo, T. Baudin, F. Brisset, T.G. Langdon, Evolution of strength and homogeneity in a magnesium AZ31 alloy processed by high-pressure torsion at different temperatures, Adv. Eng. Mater. 14 (2012) 1018-1026.

[25] K. Edalati, Z. Horita, T.G. Langdon, The significance of slippage by high-pressure torsion, Scr. Mater. 60 (2009) 9-12.

[26] R.B. Figueiredo, P.R. Cetlin, T.G. Langdon, Using finite element modeling to examine the flow processes in quasi-constrained high-pressure torsion, Mater. Sci. Eng. A 528 (2011).

[27] R.B. Figueiredoa, P.H.R. Pereira, M.T.P. Aguilar, P.R. Cetlin, T.G. Langdon, Using finite element modeling to examine the temperature distribution in quasi-constrained high-pressure torsion, Acta Mater. 60 (2012) 3190–3198.

[28] P.H.R. Pereira, R.B. Figueiredo, P.R. Cetlin, T.G. Langdon, An examination of the elastic distortions of anvils in high-pressure torsion, Mater. Sci. Eng. A 631 (2015) 201–208.

[29] D.J. Lee, E.Y. Yoon, D.H. Ahn, B.H. Park, H.W. Park, L.J. Park, Y. Estrin, H.S. Kim, Dislocation density-based finite element analysis of large strain deformation behavior of copper under high-pressure torsion, Acta Mater. 76 (2014) 281 – 293.

[30] Y. Todaka, M. Umemoto, A. Yamazaki, J. Sasaki, K. Tsuchiya, Influence of High-Pressure Torsion Straining Conditions on Microstructure Evolution in Commercial Purity Aluminum, Mater. Trans. 49 (2008) 7-14.

[31] A.Z. Zhilyaev, S. Lee, G.V. Nurislamova, R.Z. Valiev, T.G. Langdon, Microhardness and microstructural evolution in pure nickel during high-pressure torsion, Scr. Mater. 44 (2001) 2753-2758.

[32] C. Xu, Z. Horita, T.G. Langdon, Evaluating the influence of pressure and torsional strain on processing by high-pressure torsion, J. Mater. Sci. 43 (2008) 7286-7292.

[33] P.H.R. Pereira, R.B. Figueiredo, P.R. Cetlin, T.G. Langdon, Using finite element modelling to examine the flow process and temperature evolution in HPT under different constraining conditions, IOP Conf. Series: Mater. Sci. Eng. 63 (2014) 012041 (1-10).

[34] C. Xu, T.G. Langdon, Influence of a round corner die on flow homogeneity in ECA pressing, Scr. Mater. 48 (2003) 1-4.

[35] M. Kawasaki, B. Ahn, H.J. Lee, A.P. Zhilyaev, T.G. Langdon, Using high-pressure torsion to process an aluminium-magnesium nanocomposite through diffusion bonding, J. Mater. Res. 31 (2016) 88-99.

[36] A. Loucif, R.B. Figueiredo, M. Kawasaki, T. Baudin, F. Brisset, R. Chemam, T.G. Langdon, Effect of aging on microstructural development in an Al-Mg-Si alloy processed by high-pressure torsion, J. Mater. Sci. 47 (2012) 7815-7820.

[37] R.M. Molak, K. Paradowski, T. Brynk, L. Ciupinski, Z. Pakiela, K.J. Kurzydlowski, Measurement of mechanical properties in a 316L stainless steel welded joint, Int. J Pres. Ves. Pip. 86 (2009) 43–47.

[38] H.J. Lee, J.K. Han, S, Janakiraman, B. Ahn, M. Kawasaki, T.G. Langdon, Significance of grain refinement on microstructure and mechanical properties of an Al-3% Mg alloy processed by high-pressure torsion, J. Alloys Compd. 686 (2016) 998-1007.

[39] G.T. Gray, Deformation twinning in Al-4.8 wt% Mg, Acta Metall. Mater. 36 (1988) 1745–1754.

[40] X. Yang, S. Ni, M. Song, Partial dislocation emission in a superfine grained Al–Mg alloy subject to multi-axial compression, Mater. Sci. Eng. A 641 (2015) 189–193.

[41] Y. Iwahashi, Z. Horita, M. Nemoto, T.G. Langdon, Factors influencing the equilibrium grain size in equal-channel angular pressing: Role of Mg additions to aluminum, Metall. Mater. Trans. A 29A (1998) 2503-2510.

[42] M. Furukawa, Z. Horita , M. Nemoto, R.Z. Valiev, T.G. Langdon, Properties of an Al–1% Mg alloy processed by high pressure torsion, Philos. Mag. A 78 (1998) 203-216.

[43] M.A. Munnoz-Morris, C.G. Oca, D.G. Morris, Mechanical behaviour of dilute Al–Mg alloy processed by equal channel angular pressing, Scripta Mater. 48 (2003) 213–218.

[44] R. Kapoor, N.Kumar, R.S.Mishra, C.S.Huskamp, K.K.Sankaran, Influence of fraction of high angle boundaries on the mechanical behavior of an ultrafine grained Al–Mg alloy Mater. Sci. Eng. A 527 (2010) 5246-5254.

[45] J. Zhang, M.J. Starink, N. Gao, W. Zhou, Effect of Mg addition on strengthening of aluminium alloys subjected to different strain paths in high pressure torsion, Mater. Sci. Eng. A 528 (2011) 2093–2099.

[46] T.D. Topping, B. Ahn, Y. LI, S.R. Nutt, E.J. Lavernia, Influence of Process Parameters on the Mechanical Behavior of an Ultrafine-Grained Al, Alloy Metall. Mater. Trans. A 43 (2012) 505-519.

[47] M.P. Liu, H.J. Roven, M.Yu. Murashkin, R.Z. Valiev, A. Kilmametov, Z. Zhang, Y. Yu, Structure and mechanical properties of nanostructured Al–Mg alloys processed by severe plastic deformation, J. Mater. Sci. 48 (2013) 4681–4688.

[48] S. Zhao, C. Meng, F. Mao, W. Hu, G. Gottstein, Influence of severe plastic deformation on dynamic strain aging of ultrafine grained Al–Mg alloys, Acta Mater. 76 (2014) 54-67.

[49] S.-Y. Chang, B.-D. Ahn, S.-K. Hong, S. Kamado, Y. Kojima, D.H. Shin, Tensile deformation characteristics of a nano-structured 5083 Al alloy, J. Alloys Compd. 386 (2005) 197–201.

[50] A.A. Mazilkina, B.B. Straumal, E. Rabkin, B. Baretzky, S. Enders, S.G. Protasova, O.A. Kogtenkova, R.Z. Valiev, Softening of nanostructured Al–Zn and Al–Mg alloys after severe plastic deformation Acta Mater. 54 (2006) 3933-3939.

[51] V.L. Tellkamp, E.J. Lavernia, A. Melmed, Mechanical behavior and microstructure of a thermally stable bulk nanostructured Al alloy, Metall. Mater. Trans. A 32 (2001) 2335-2343.

[52] Z. Lee, F. Zhou, R.Z. Valiev, E.J. Lavernia, S.R. Nutt, Microstructure and microhardness of cryomilled bulk nanocrystalline Al–7.5%Mg alloy consolidated by high pressure torsion, Scripta Mater. 51 (2004) 209-214.

[53] K.M. Youssef , R.O. Scattergood, K.L. Murty, C.C. Koch, Nanocrystalline Al–Mg alloy with ultrahigh strength and good ductility, Scripta Mater. 54 (2006) 251-256.

[54] P. Bazarnik, M. Lewandowska, M. Andrzejczuk, K.J. Kurzydlowski, The strength and thermal stability of Al-5Mg alloys nano-engineered using methods of metal forming, Mater. Sci. Eng. A 556 (2012) 134-139.

[55] M.R. Toroghinejad, F. Ashrafizadeh, R. Jamaati, On the use of accumulative roll bonding process to develop nanostructured aluminum alloy 5083, Mater. Sci. Eng. A 561 (2013) 145–151.

[56] M. Zha, Y. Li, R.H. Mathiesen, R. Bjørge, H.J. Roven. Microstructure, hardness evolution and thermal stability of binary Al-7Mg alloy processed by ECAP with intermediate annealing, T. Nonferrous Met. Soc. China 24 (2014) 2301-2306.

[57] Y.Z. Tian, S.D. Wu, Z.F. Zhang, R.B. Figueiredo, N. Gao, T.G. Langdon, Comparison of microstructures and mechanical properties of a Cu–Ag alloy processed using different severe plastic deformation modes, Mater. Sci. Eng. A 528 (2011) 4331–4336.

[58] R.B. Figueiredo, T.G. Langdon, Heterogeneous flow during high-pressure torsion, Mater. Res. 16 (2013) 571-576.

[59] Y. Huang, M. Kawasaki, A. Al-Zubaydi, T.G. Langdon, Effect of anvil roughness on the flow patterns and hardness development in high-pressure torsion, J. Mater. Sci. 49 (2014) 6517-6528.

[60] M.J. Zehetbauer, H.P. Stuwe, A. Vorhauer, E. Schafler, J. Kohout, The Role of Hydrostatic Pressure in Severe Plastic Deformation, Adv. Eng. Mater. 5 (2003) 330-337.

[61] A.T. Krawczynska, T. Brynk, S. Gierlotka, E. Grzanka, S. Stelmakh, B. Pałosz, M. Lewandowska, K.J. Kurzydłowski, Mechanical properties of nanostructured stainless steel 316LVM annealed under pressure, Mech. Mater. 67 (2013) 25-32.

[62] H.L.D. Pugh, *Mechanical Behaviour of Materials Under Pressure*, Elsevier, Amsterdam (1970).

[63] R.Ye. Lapovok, The role of back-pressure in equal channel angular extrusion, J. Mater. Sci. 40, (2005) 341–346.

Figure captions

Fig. 1 Schematic illustration of tensile specimen cut from the off-centre positions.

Fig. 2 Variation of hardness with distance from the disc centre for samples processed under pressures of 1.0 and 6.0 GPa.

Fig. 3 Color-coded contour maps showing the Vickers microhardness across the surfaces of discs processed by HPT through different numbers of turns under pressures of (a) 1.0 and (b) 6.0 GPa.

Fig. 4 Distribution of Vickers microhardness as a function of location along the one-half cross-section of discs processed by HPT through different numbers of turns under pressures of 1.0 and 6.0 GPa.

Fig. 5 Representative bright field images in TEM with the corresponding SAED patterns of samples processed by HPT through 1/2 and 5 revolutions under applied pressures of 1.0 and 6.0 GPa.

Fig. 6 TEM images of central regions in samples processed by one HPT revolution under applied pressures of (a) 1.0 and (b) 6.0 GPa.

Fig. 7 Plots of stress versus strain for tensile specimens processed by HPT through different numbers of turns under pressures of (a) 1.0 and (b) 6.0 GPa.

Fig. 8 The Hall-Petch relationship after HPT processing together with experimental data for other Al-xMg alloys using data summarized in Table 3 [3,41-56]

Table captions

Table 1 Average grain size in sections parallel to the disc planes: data from centres and edges measured for both applied pressures.

Table 2 Mechanical properties determined in tensile tests.

Table 3 Grain size and mechanical properties of Al-xMg alloys processed by various SPD procedures [3,41-56].

Table 1 Average grain size in sections parallel to the disc planes: data from centres and edges measured for both applied pressures.

Pressure (GPa)	Location	Number of revolutions 1/4	1/2	1	3	5
1.0	Centre (nm)	-	-	-	310	250
	Edge (nm)	200	170	140	135	110
6.0	Centre (nm)	-	-	-	285	235
	Edge (nm)	175	155	135	130	120

Table 2 Mechanical properties determined in tensile tests

Pressure (GPa)	Location	Number of revolutions 1/4	1/2	1	3
1.0	UTS [MPa]	490	510	560	830
	YS [MPa]	400	420	470	560
6.0	UTS [MPa]	500	600	700	850
	YS [MPa]	450	460	570	600

Table 3 Grain size and mechanical properties of Al-xMg alloys processed by various SPD procedures [3,41-56].

Aluminium alloy	Processing history	Grain size (nm)	UTS (MPa)	YS (MPa)	Microhardness (MPa)	Ref.
Polycrystalline Al-5483	-	10000	360	145	880	-
Al-0.5Mg	HPT 6 GPa	265	490	390	1038	Liu et al., 2013
Al-1Mg	ECAP 6p (B)	450	285	250	-	Iwahashi et al., 1998
Al-1Mg	CCDP 18p	250	-	200	-	Zhao et al. 2014
Al-1Mg	HPT 3 GPa (16t)	210	-	-	1860	Zhang et al. 2011
Al-1Mg	HPT 6 GPa (10t)	230	440	400	1140	Huang et al., 2014
Al-2.5Mg	ECAP 4p (A)	1470	267	222	-	Kapoor et al., 2010
Al-2.5Mg	HPT 6 GPa	86	670	505	1650	Liu et al., 2013
Al-3Mg	ECAP 4p	200	400	370	-	Furukawa et al. 1998
Al-3Mg	ECAP 8p (A)	250	510	392	1100	Munnoz-Morris et al., 2003
Al-3Mg	ECAP 8p (B)	270	460	420	-	Iwahashi et al., 1998
Al-3Mg	CCDP 18p	200	-	350	-	Zhao et al. 2014
Al-3Mg	HPT 3 GPa (16t)	150	-	-	2300	Zhang et al. 2011
Al-4,5Mg	Quasi-Isostatic Forging 523K	193	598	521	1620	Topping et al., 2012
Al-5182	HPT 6 GPa	71	800	690	1867	Liu et al., 2013
Al-5Mg	Cryo-milling + consolidation	26	742	620	2300	Youssef et al., 2006
Al-5083	Cryo-milling + consolidation	Bimodal	462	334	-	Tellkamp et al., 2004
Al-5483	Plastic consolidation of powders at 753K	450	470	400	1275	Bazarnik et al. 2012
Al-5083	ECAP 373K 8p (C)	500	430	400	-	Chang et al. 2005
Al-5Mg	CCDP 18p	100	-	475	-	Zhao et al. 2014
Al-5083	ARB	80 – layer thickness	-	550	1570	Toroghinejad et al., 2013
Al-5Mg	HPT 5 GPa (5t)	150	-	-	2070	Mazilkina et al., 2006
Al-5483	HE	190	520	475	1410	Bazarnik et al. 2013
Al-5483	ECAP + HE	100	595	560	1755	Bazarnik et al. 2013
Al-7Mg	ECAP 6p (B_c)	150	600	538	-	Zha et al., 2014
Al-7,5Mg	Cryo-milling + HPT consolidation	20	-	-	3800	Zhou et al., 2004
	Cryo-milling + HIP consolidation	200	-	-	2000	
Al-10Mg	HPT 5 GPa (5t)	90	-	-	2800	Mazilkina et al., 2006
Al-5483	HPT 6 GPa (3t)	130	850	600	2000	This Study

Re: CCDP - Confined channel-die pressing, HE – Hydrostatic Extrusion, ECAP – Equal Channel Angular Pressing, ARB – Accumulative Roll Bonding, HIP – High Isotactic Pressing

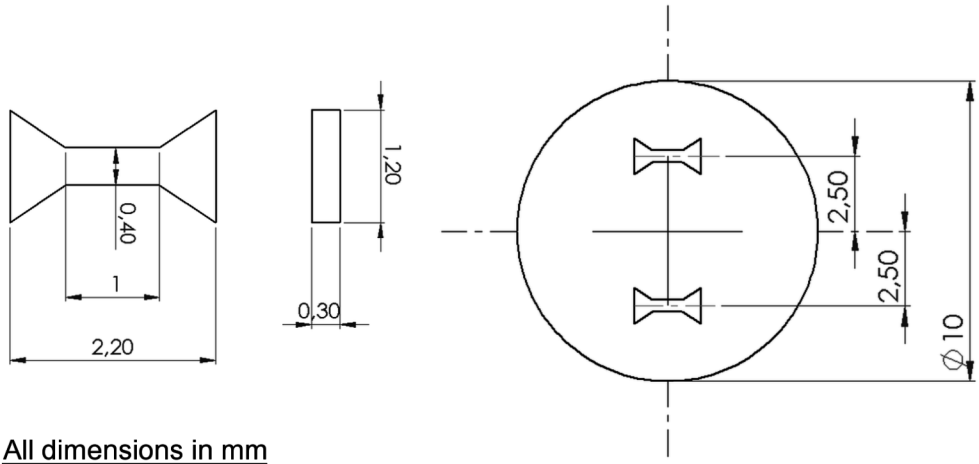

All dimensions in mm

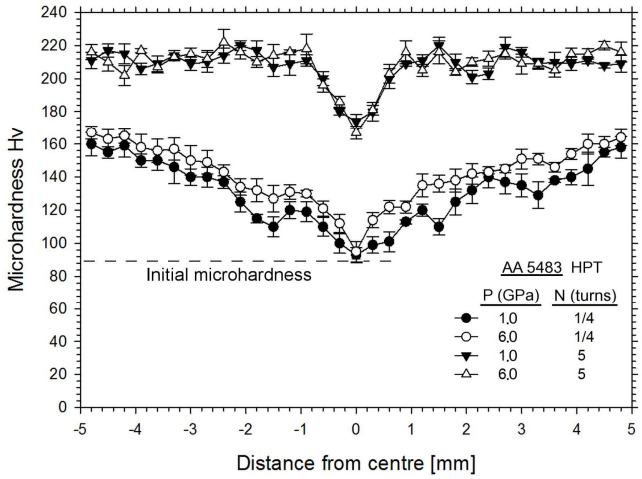

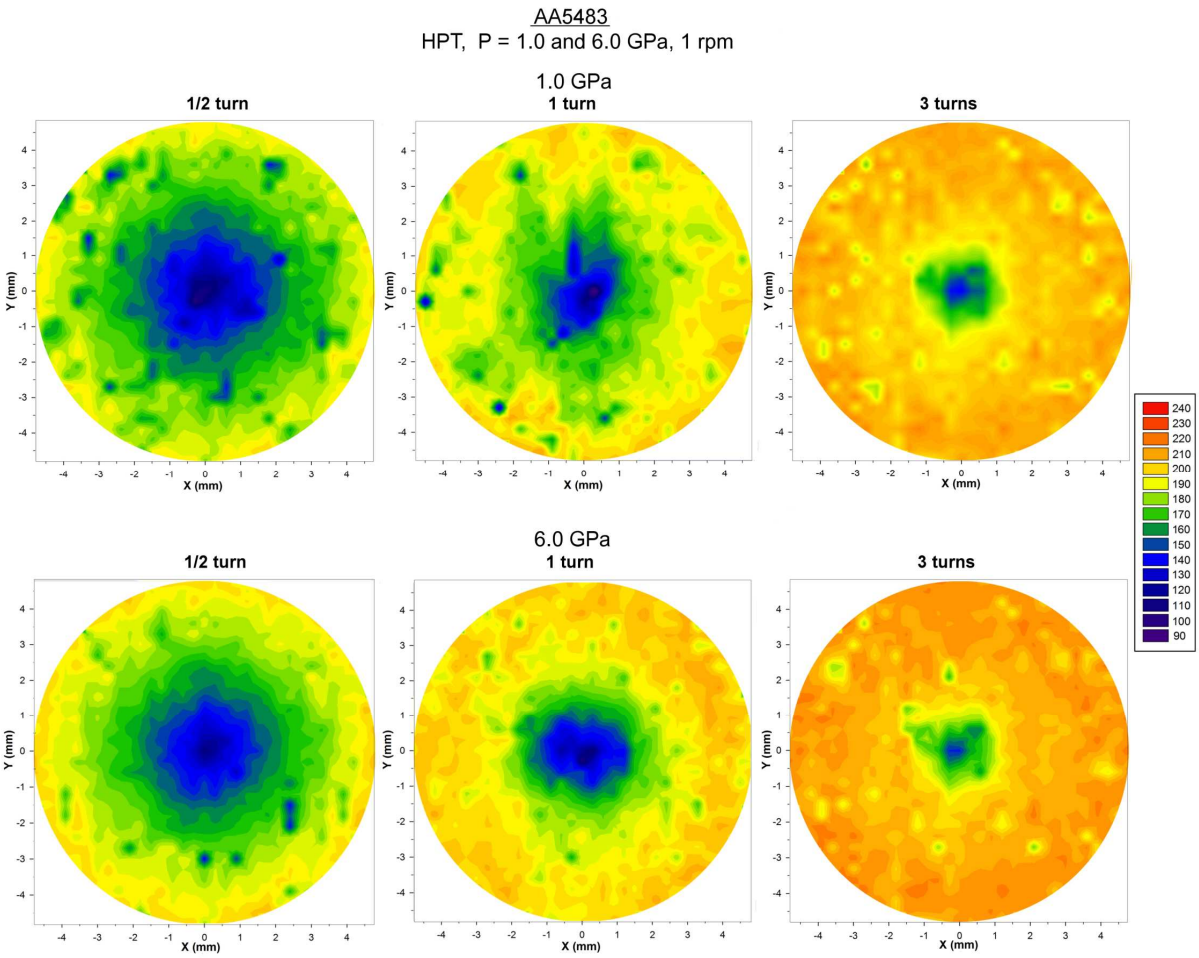
AA5483
HPT, P = 1.0 and 6.0 GPa, 1 rpm
1.0 GPa
1/2 turn
1 turn
3 turns
6.0 GPa
1/2 turn
1 turn
3 turns
Y (mm)
X (mm)
240
230
220
210
200
190
180
170
160
150
140
130
120
110
100
90

AA5483
HPT, P = 1.0 and 6.0 GPa, 1 rpm

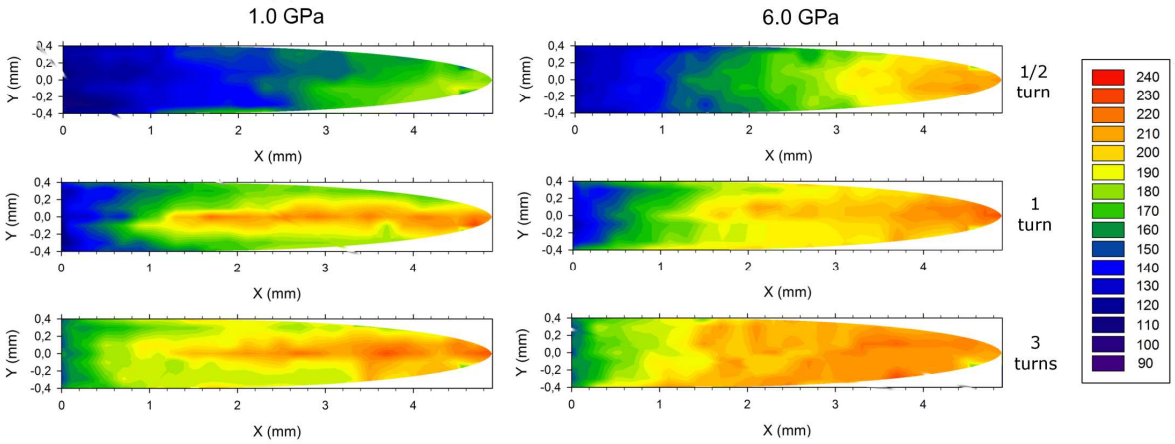

AA5483
HPT, P = 1.0 and 6.0 GPa, 1 rpm

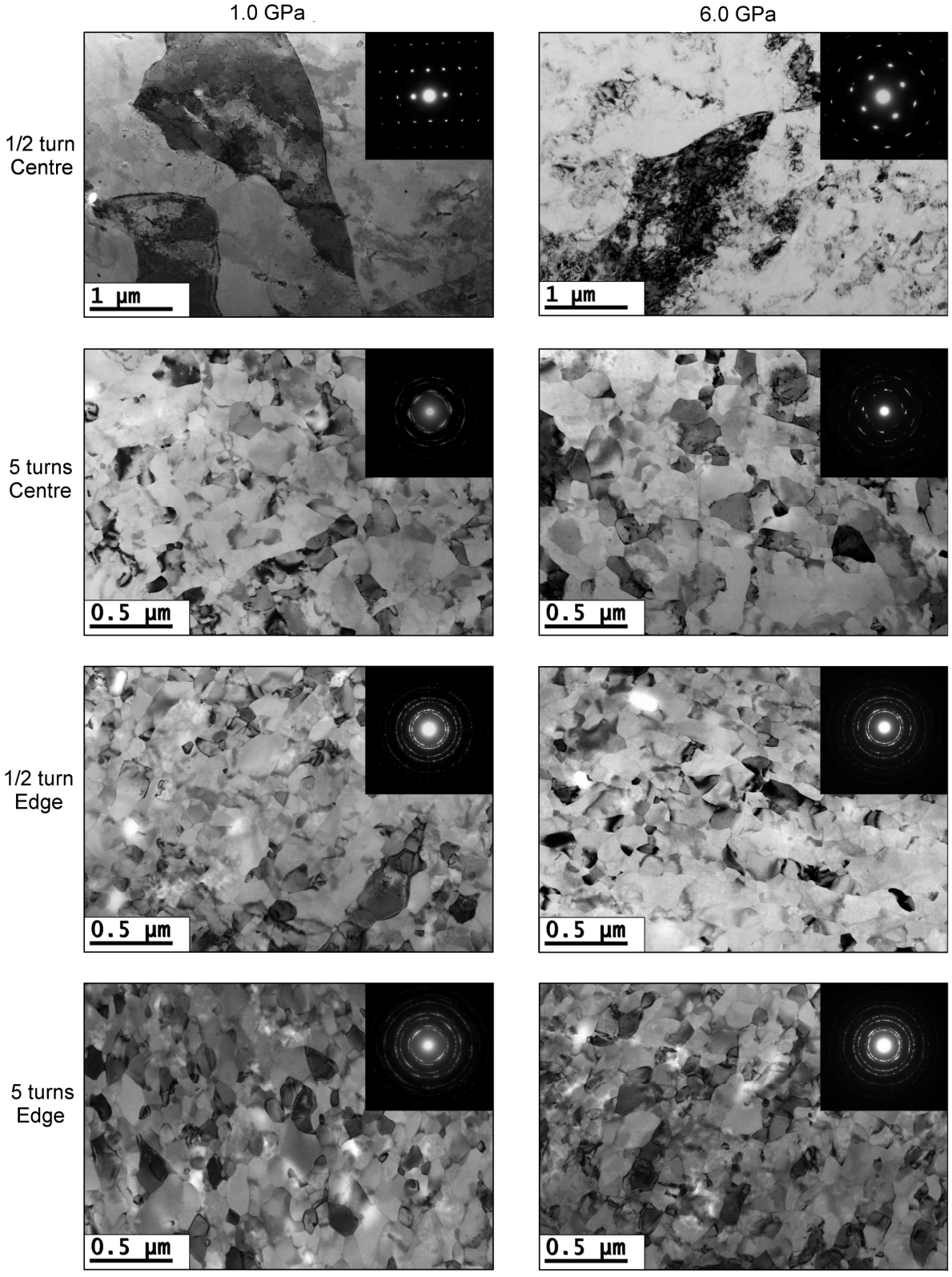

1.0 GPa

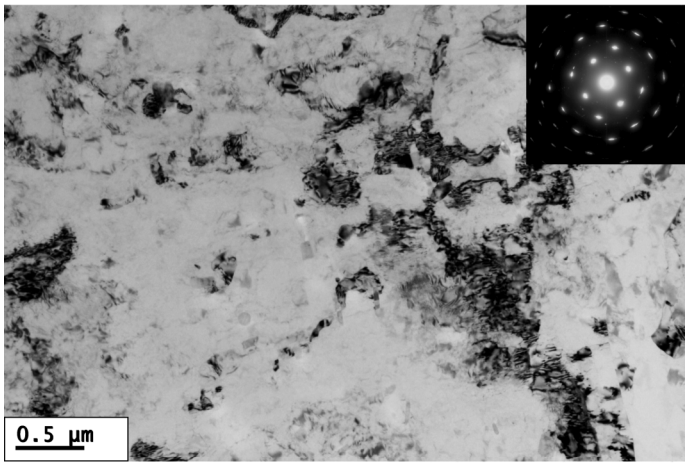

6.0 GPa

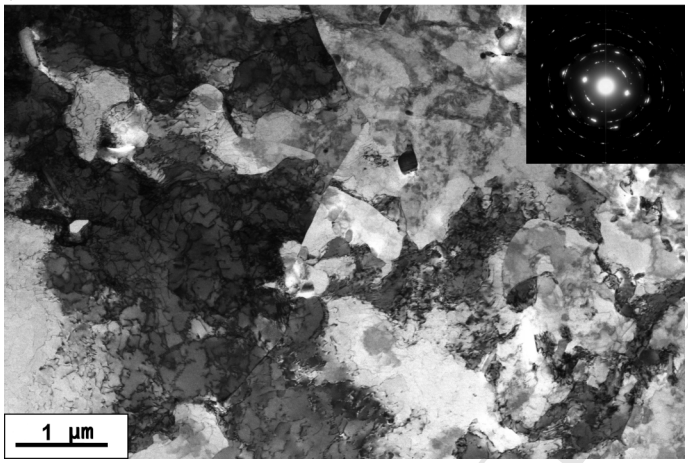

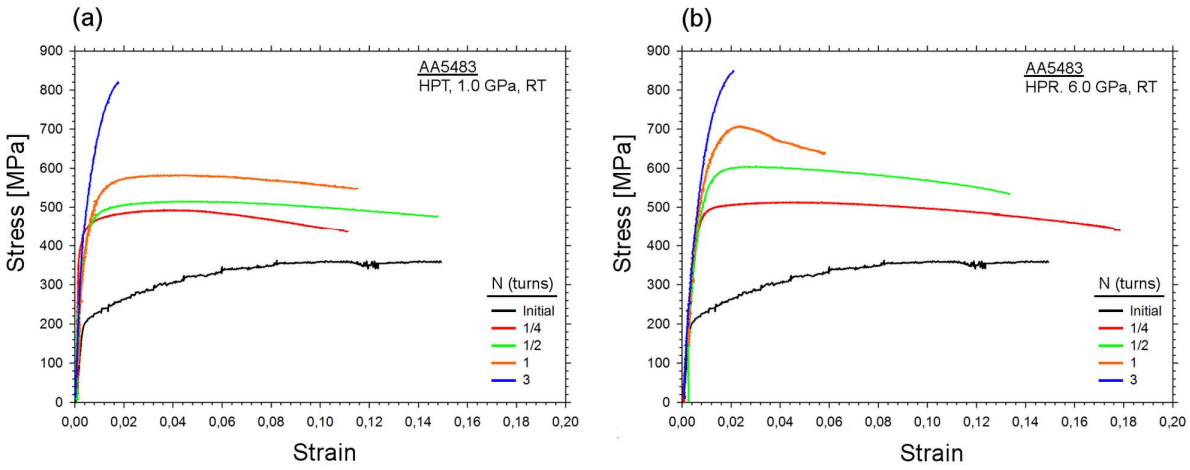

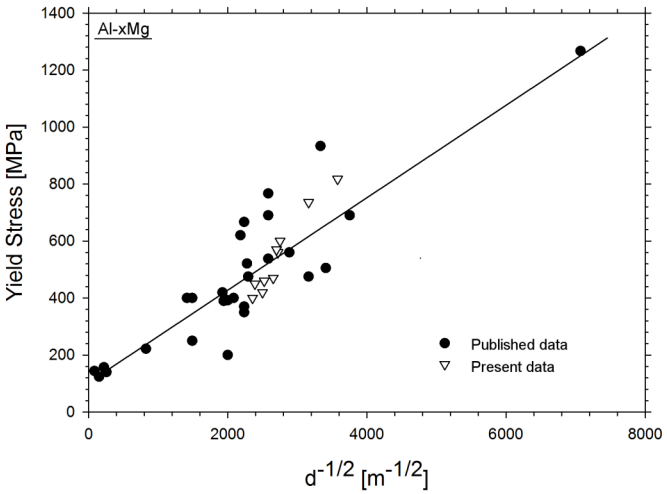

Highlights

- AA5483 alloy was processed by HPT under two different pressures of 1 and 6 GPa
- In both types of samples UFG structure was achieved after 5 revolutions
- The microstructure and hardness evolution is influenced by the applied pressure
- The effect of pressure is especially visible up to one turn
- At higher numbers of turns, the microstructure and properties tend to homogenize